Ruthenium complex, TQ-5, protects against LPS-induced macrophage inflammation and acute liver injury in mice via downregulating NF-κB pathways

SHAW-MIN HOU[1-3*], CHIH-HSUAN HSIA[3,4*], MARAPPAN VELUSAMY[5], THANASEKARAN JAYAKUMAR[3], CHIH-WEI HSIA[3], CHAO-CHIEN CHANG[1-3], KUAN-HUNG LIN[6] and YUNG-CHANG LU[6,7]

[1]Cardiovascular Center, Cathay General Hospital, Taipei 106; [2]Division of Cardiovascular Surgery, Department of Surgery, School of Medicine, College of Medicine, Fu Jen Catholic University, New Taipei City 242; [3]Graduate Institute of Medical Sciences, College of Medicine, Taipei Medical University, Taipei 110; [4]Central Laboratory, Shin-Kong Wu Ho-Su Memorial Hospital, Taipei 111, Taiwan, R.O.C.; [5]Department of Chemistry, North Eastern Hill University, Shillong 793022, India; [6]Institute of Biomedical Sciences and Department of Medicine, Mackay Medical College, New Taipei City 252; [7]Department of Orthopedic Surgery, Mackay Memorial Hospital, Taipei 104, Taiwan, R.O.C.

Received November 2, 2018; Accepted April 19, 2019

DOI: 10.3892/ijmm.2019.4179

Abstract. A newly synthesized ruthenium metal complex, TQ-5, exhibited antithrombotic and antiplatelet effects in our previous study. In the present study, the anti-inflammatory/hepatoprotective effects and mechanisms of action of TQ-5 were investigated in lipopolysaccharide (LPS)-induced RAW 264.7 macrophages *in vitro* and in acute liver injury in mice *in vivo*. The results demonstrated that TQ-5 suppressed the LPS-induced production of nitric oxide, tumor necrosis factor-α (TNF-α), interleukin-1β (IL-1β) and inducible nitric oxide synthase (iNOS), without inducing cytotoxicity or damaging the morphology of the RAW 264.7 macrophages. In addition, the role of TQ-5 in mediating mitogen-activated protein kinases and nuclear factor κB (NF-κB) pathways involved in the inflammation process of LPS-stimulated RAW264.7 cells was investigated. Although TQ-5 did not alter the phosphorylation of extracellular signal-related kinase, p38 or c-Jun N-terminal kinase in LPS-treated cells, it suppressed the phosphorylation of Akt in a concentration-dependent manner. TQ-5 significantly reversed the LPS-induced degradation of inhibitor of NF-κBα and phosphorylation of p65. The mRNA expression levels of iNOS, TNF-α and IL-1β were also suppressed by TQ-5. TQ-5 improved LPS-induced liver injury in mice by inhibiting the expression of TNF-α, IL-1β and iNOS and phosphorylation of NF-κBp65. These findings suggest that Akt/NF-κB signaling may be a promising target for TQ-5 to combat LPS-induced inflammation. Therefore, TQ-5 may act as a potential agent for the development of anti-inflammatory drugs to treat acute liver failure.

Correspondence to: Dr Yung-Chang Lu, Department of Orthopedic Surgery, Mackay Memorial Hospital, 92, Section 2, Zhongshan North Road, Taipei 104, Taiwan, R.O.C.
E-mail: yungchanglu@hotmail.com

*Contributed equally

Key words: RAW 264.7 cell, ruthenium metal complex, lipopolysaccharide, nuclear factor-κB/Akt, mouse liver injury

Introduction

Inflammatory cells, such as macrophages and microglia, are activated and accumulate in heart and brain tissues following ischemic onset, causing inflammatory injury (1). Acute liver failure is a life-threatening disease with a high mortality rate worldwide and a substantial impact on public health (2). This disease is characterized by hepatic dysfunction, irregular liver biochemical values and coagulopathy. It is associated with rapidly enlightened multiple organ failure, which can have devastating consequences. The current methods for diagnosing acute liver failure are underdeveloped; liver transplantation is the most common treatment strategy (3). Therefore, there is an unmet medical need to develop novel therapeutic strategies for acute liver failure. Acute liver failure is caused by inflammation-mediated hepatocellular injury, which strictly resembles the innate immune response induced by exposure to lipopolysaccharide (LPS). The LPS-induced acute liver injury model is a well-established animal model that may precisely mimic clinical indicators in humans (4). LPS induces Kupffer cell activation via the Toll-like receptor 4 signaling pathway, activates nuclear factor (NF)-κB, and recruits the release of inflammatory cytokines, including interleukin (IL)-1β, IL-6 and tumor necrosis factor (TNF)-α (5). As the same inflammatory mediators appear to be associated with the pathogenesis of acute liver injury, their inhibition is essential for developing

therapeutic strategies, which can be evaluated in animal models of LPS-induced liver failure.

The mitogen-activated protein kinase (MAPK) signaling pathway is reported to be involved in proinflammatory responses in LPS-induced macrophages (6). Three major MAPK families have been recognized, including extracellular signal-related kinase (ERK), p38 and c-Jun N-terminal kinase (JNK). ERK stimulation is associated with the LPS-induced production of TNF-α in macrophages (7). In addition, the triggering of p38 is involved in the production of inflammatory stimulators for leucocyte recruitment and activation, and p38 controls the expression of several inflammation-related genes, including TNF-α and IL-6 (8,9). Furthermore, JNK is induced by bacterial endotoxins, inflammatory cytokines, hypoxia and ultraviolet radiation (10). Therefore, suppression of the MAPK pathway may reveal the anti-inflammatory activities of drugs. NF-κB is a transcription factor that has a significant contribution in inflammation (11), and NF-κB is composed of p65 and p50 subunits. In normal unstimulated cells, NF-κB is present in a stable form in the cytosol as the inhibitor of NF-κB (IκB)-NF-κB complex. Following LPS stimulation, IκB is activated by the degradation and phosphorylation of IκB via IκB kinase (IKK). This phosphorylation results in the detachment of IκB from the IκB-NF-κB complex, thereby enabling NF-κB to translocate to the nucleus and triggering the transcription of proinflammatory genes, including inducible nitric oxide synthase (iNOS), TNF-α and IL-6 (12). By contrast, the Akt pathway regulates cellular activation, inflammatory responses and apoptosis (13). A previous study established that the Akt pathway executes a decelerating mechanism to control proinflammatory mediators in LPS-induced microglia by inhibiting the JNK and p38 MAPK pathways (14). Therefore, an inhibitor of NF-κB/Akt may be active as an anti-inflammatory agent.

Metal complexes are useful resources for drug design due to their potential mechanisms of action. A large group of metal-based drugs have been designed for their various oxidation states and overall coordination geometries (15,16). The application of metal complexes in medicine has recently been stimulated due to the clinical success of anticancer cisplatin and other platinum (II) compounds. Furthermore, the high structural diversity of metal complexes is an attractive platform for designing drugs for other conditions, including neurodegeneration, microbial and parasitic infections and inflammation (17). In our previous study, a substantial number of ruthenium metal compounds were identified as being effective antiplatelet agents for the prevention and treatment of thrombotic diseases (18,19). Therefore, it is clear that metal complexes have the potential to offer an alternative to anti-inflammatory organic drugs. The present study aimed to investigate the ability of a novel ruthenium-based metal complex, TQ-5, on inhibiting the LPS-induced expression of iNOS and subsequent production of TNF-α, nitric oxide (NO) and IL-1β in RAW 264.7 macrophage cells and in mouse liver injury models. In addition, the study aimed to clarify the underlying protective mechanisms of TQ-5 in a mouse liver injury model by investigating the involvement of NF-κB, MAPK and Akt signaling molecules.

Materials and methods

Chemicals and reagents. Fetal bovine serum (FBS), Dulbecco's modified Eagle's medium (DMEM), L-glutamine penicillin/streptomycin, and anti-α-tubulin (cat. no. MS-581-P1) monoclonal antibodies (mAbs) were purchased from Invitrogen (Thermo Fisher Scientific, Inc., Waltham, MA, USA). LPS (*Escherichia coli* 0127:B8), 3-(4,5-dimethylthiazol-2-yl)-2,5-diphenyltetrazolium bromide (MTT), and dimethyl sulfoxide (DMSO) were purchased from Sigma-Aldrich (St. Louis, MO, USA). Anti-iNOS (cat. no. sc-650) polyclonal antibody (pAb) was purchased from Santa Cruz Biotechnology, Inc. (Dallas, TX, USA). Anti-TNF-α (cat. no. 3707), anti-JNK (cat. no. 9252), anti-phospho-c-JNK (Thr183/Tyr185; cat. no. 9251), anti-phospho-p44/p42 ERK (Thr202/Tyr204; cat. no. 9101), anti-phospho-p38 MAPK (Thr180/Tyr182; cat. no. 9211), anti-phospho-Akt (cat. no. 9271) pAbs, anti-phospho-p65 (Ser536; cat. no. 3033), anti-p65 (cat. no. 4764), anti-IκBα (cat. no. 4812), anti-ERK (cat. no. 9107), anti-Akt (cat. no. 2920), and anti-p38 MAPK (cat. no. 9217) mAbs were purchased from Cell Signaling Technology, Inc. (Danvers, MA, USA). Anti-IL-1β (cat. no. 5128) pAb was purchased from BioVision, Inc. (Milpitas, CA, USA). Horseradish peroxidase (HRP)-conjugated donkey anti-rabbit immunoglobulin G (IgG; cat. no. RPN4301) and sheep anti-mouse IgG (cat. no. RPN4201) were purchased from Amersham; GE Healthcare Life Sciences (Chalfont, UK). Western blotting detection reagent for enhanced chemiluminescence (ECL) and Hybond™-P polyvinylidene difluoride (PVDF) blotting membranes were purchased from GE Healthcare Life Sciences.

TQ-5 synthesis and RAW 264.7 cell cultivation. The ruthenium metal complex TQ-5 and its ligand (L) were synthesized according to the method described in our previous study (18). The RAW 264.7 cells were obtained from ATCC (cat. no. TIB-71) and cultured in DMEM supplemented with 10% FBS and 100 U/ml penicillin G and 100 mg/ml streptomycin at 37˚C in a humidified atmosphere of 5% CO_2/95% air (20).

Cell viability assay. The RAW 264.7 cells ($2x10^5$ cells per well) were seeded into 24-well culture plates with DMEM containing 10% FBS for 24 h. The cells were treated with various concentrations of TQ-5 (10, 20 and 40 μM) or solvent control (0.1% DMSO) for 20 min and then stimulated with LPS (1 μg/ml) or left unstimulated for 24 h at 37˚C. Cell viability was measured using an MTT assay (20). The cell viability index was calculated as follows: (absorbance of treated cells/absorbance of control cells) x100%. The absorbance of samples was determined at 570 nm using an MRX absorbance reader (Dynex Technologies, Chantilly, VA, USA).

Determination of NO production. To determine NO production, the content of nitrite/nitrate, as stable oxidative end products of NO, was measured as previously described (20) with minor modifications. The RAW 264.7 cells were seeded into 6-cm dishes ($8x10^5$) with DMEM containing 10% FBS for 24 h. The cells were treated with TQ-5 (10-40 μM) or solvent control (0.1% DMSO) for 20 min and then stimulated with LPS (1 μg/ml) or left unstimulated for 24 h. These conditioned

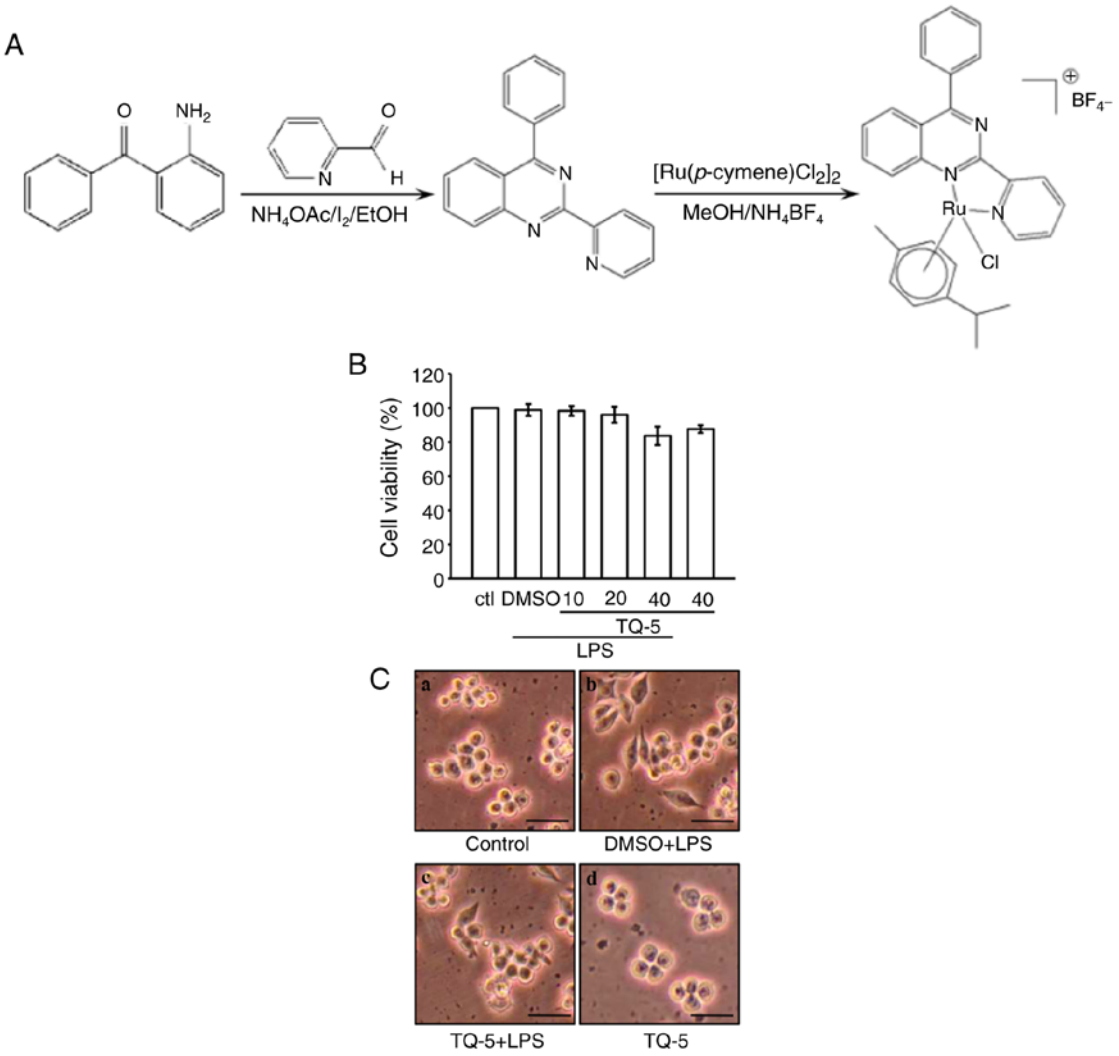

Figure 1. Effect of TQ-5 on the viability and morphology of LPS-stimulated RAW cells. (A) Chemical structures of TQ-5. Cell viability was measured using a 3-(4,5-dimethylthiazol-2-yl)-2,5-diphenyltetrazolium bromide assay (B); cells were pretreated with various concentrations of TQ-5 (10, 20 and 40 μM) for 20 min and then treated with LPS (1 μg/ml) for 24 h. Cell morphology was observed using optical microscopy (C-a) solvent control (0.1% DMSO), (C-b) DMSO with LPS (1 μg/ml), (C-c) TQ-5 (40 μM) with LPS, and (C-d) TQ-5 only. Scale bar=50 μm. Arrows indicate activated cells. LPS, lipopolysaccharide; DMSO, dimethyl sulfoxide; ctl, control.

supernatants were collected and mixed with equal volumes of Griess reagent. The absorbance of samples was determined at 550 nm by using an MRX absorbance reader. The concentrations of nitrite/nitrate were calculated using a standard curve through linear regression of absorbance measurements of standard solutions (sodium nitrite dissolved in the same culture medium).

Reverse transcription-quantitative polymerase chain reaction (RT-qPCR) analysis. Total RNA was extracted from the RAW 264.7 cells using the NucleoSpin® RNA kit (Macherey-Nagel, Düren, Germany). RT-qPCR analysis was performed using Fast SYBR®-Green Master mix (Thermo Fisher Scientific, Inc.), following the manufacturer's instructions, to determine the expression of target genes, and the results were normalized using the expression of glyceraldehyde 3-phosphate dehydrogenase (GAPDH). Amplification was performed using a StepOne Real-Time PCR system (Applied Biosystems; Thermo Fisher Scientific, Inc.). The cycling conditions were as follows: Hot-start activation at 95˚C for 20 sec followed by 40 cycles of denaturation at 95˚C for 3 sec and annealing/extension at 60˚C for 30 sec. The following primers were used in the present study: TNF-α, forward 5'-TCTTCTGTCTACTGAACTTCGG-3' and reverse 5'-AAGATGATCRGAGTGTGAGGG-3'; IL-1β, forward 5'-AACCTGCTGGTGTGTGACGTTC-3' and reverse 5'-CAGCACGAGGCTTTTTTGTTGT-3'; iNOS, forward 5'-CGAAACGCTTCACTTCCAA-3' and reverse 5'-TGAGCCTATATTGCTGTGGCT-3'; and GAPDH, forward 5'-GAACATCATCCCTGCATCCA-3' and reverse 5'-GCCAGTGAGCTTCCCGTTC-3'. Densitometry quantification was performed using the comparative CT method ($2^{-\Delta\Delta Cq}$) (21). Samples were normalized by GAPDH.

Animals. A total of 26 male C57BL/6 mice (22-25 g; 8 weeks old) were obtained from BioLasco Taiwan Co., Ltd. (Taipei, Taiwan). The mice were kept in cages at a temperature of 22±4˚C and a relative humidity of 50±20% under a 12 h light-dark cycle. Experimental mice received a standard pellet diet and water *ad libitum*. All animal experiments and care procedures conformed to the Guide for the Care and Use of

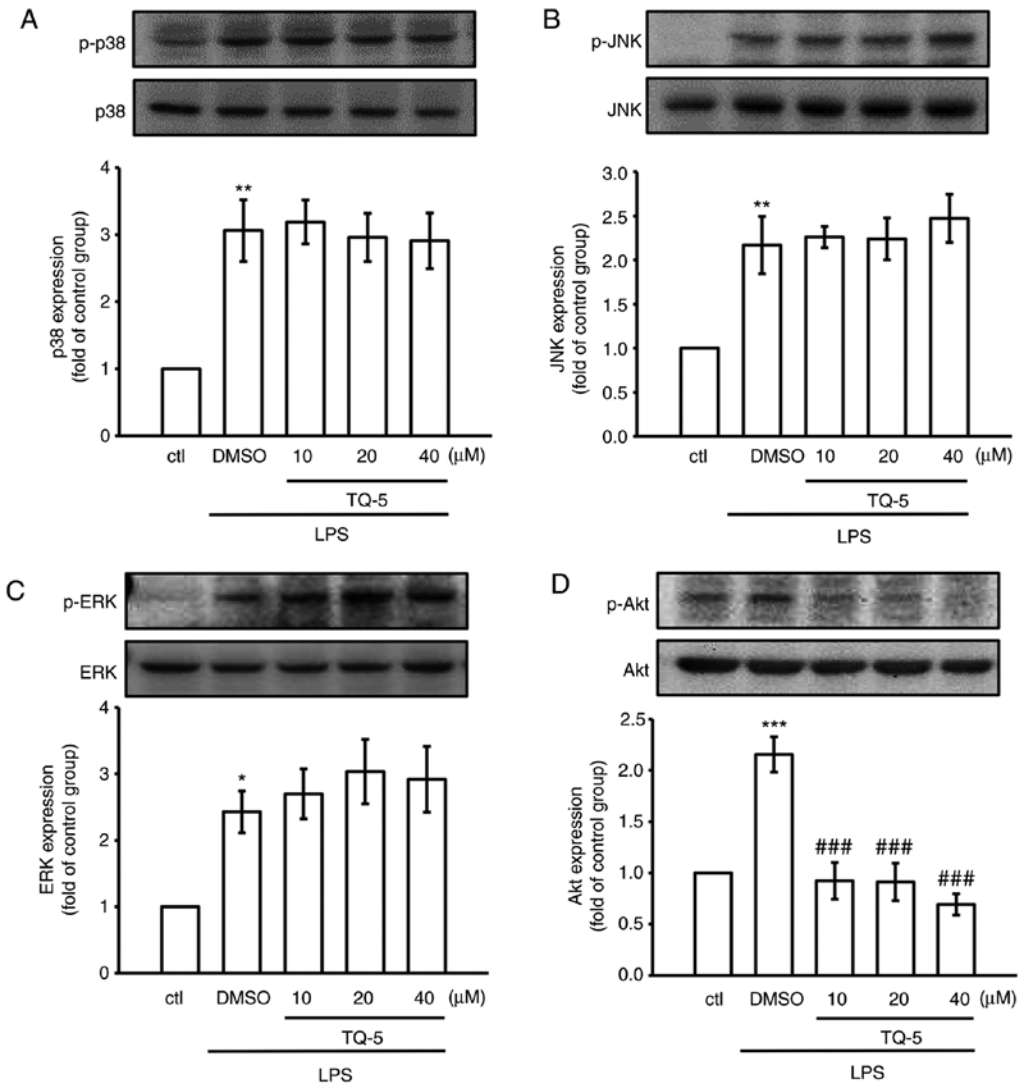

Figure 2. Effect of TQ-5 on LPS-induced MAPK and Akt signaling pathways in RAW cells. RAW cells were treated with 0.1% DMSO or various concentrations of TQ-5 (10, 20 and 40 μM) for 20 min, followed by LPS (1 μg/ml) for 30 min. The expression of phosphorylated (A) p38 MAPK, (B) JNK, (C) ERK and (D) Akt were detected by immunoblotting. Data are expressed as the mean ± SEM (n=4). *P<0.05, **P<0.01 and ***P<0.001 compared with the ctrl group; $^{###}$P<0.001 compared with the LPS group. LPS, lipopolysaccharide; MAPK, mitogen-activated protein kinase; JNK, c-Jun N-terminal kinase; ERK, extracellular signal-regulated kinase; p-, phosphorylated; DMSO, dimethyl sulfoxide; ctl, control.

Laboratory Animals (LAC-2016-0395) and were approved by the Institutional Animal Care and Use Committee of Taipei Medical University (Taipei, Taiwan).

LPS-induced acute liver inflammation in mice. The mice were divided into the following four groups: i) Control, ii) LPS (2.5 mg/kg), iii) TQ-5 (2 mg/kg) + LPS (2.5 mg/kg), and iv) TQ-5 (4 mg/kg) + LPS (2.5 mg/kg). The mice were initially pretreated intraperitoneally with TQ-5 or 0.1% DMSO, and 2 h following the administration of TQ-5, LPS was injected intraperitoneally. The mice were sacrificed following 6 h of LPS stimulation, and liver tissues were quickly removed and stored at -80˚C until analysis.

Assessment of hepatic function. The mice were sacrificed following 6 h of LPS (2.5 mg/kg) stimulation. Subsequently, blood was collected and serum was separated by centrifugation at 500 x g for 10 min at room temperature. The serum alanine aminotransferase (ALT) and aspartate aminotransferase (AST) levels were determined to assess liver function using the Vet-Test® chemistry analyzer (IDEXX, Westbrook, ME, USA). Enzyme activities are expressed as international units per liter.

Western blotting. Western blot analysis was performed in cells and liver tissue homogenates by following a previously described method (20). In brief, the RAW 264.7 cells ($8x10^5$ cells/dish) were seeded onto 6-cm dishes with DMEM containing 10% FBS for 24 h. The cells were pretreated with TQ-5 or 0.1% DMSO for 20 min and then stimulated with LPS (1 μg/ml) or left unstimulated according to the experimental design. Subsequently, the proteins from the cells and liver tissues were extracted using lysis buffer (containing 50 mM HEPES, 5 mM EDTA, 50 mM NaCl and 1% Triton X-100). The extracted protein samples (50 μg) were applied for 12% sodium dodecyl sulfate-polyacrylamide gel electrophoresis, and the separated proteins were then electrophoretically transferred onto PVDF membranes (0.45-μm). The membranes

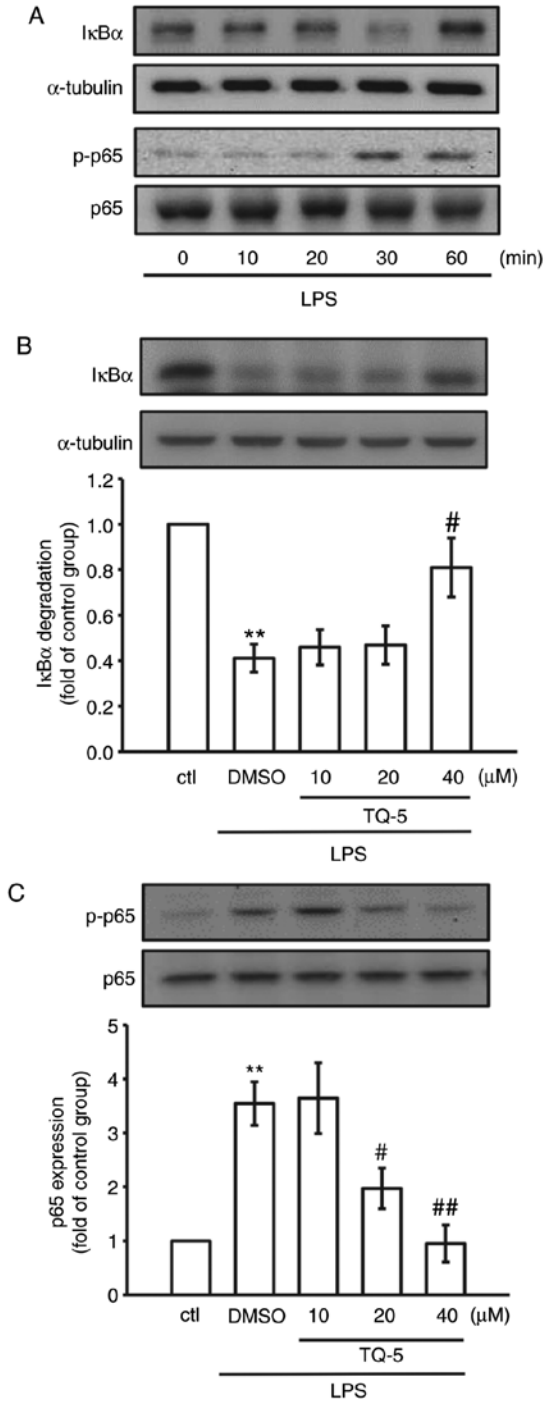

Figure 3. TQ-5 reverses LPS-induced IκBα degradation and inhibits the phosphorylation of p65 in RAW cells. (A) Cells were treated with LPS (1 μg/ml) for the indicated times (10-60 min). IκBα degradation and the phosphorylation of p65 were determined by immunoblotting. Cells were treated with 0.1% DMSO or TQ-5 (10, 20 and 40 μM) for 20 min, followed by LPS (1 μg/ml) for 30 min. (B) IκBα degradation and (C) the phosphorylation of p65 were evaluated by immunoblotting. Data are presented as the mean ± SEM (n=4). **P<0.01 compared with the ctl group; $^{\#}$P<0.05 and $^{\#\#}$P<0.01 compared with the LPS group. LPS, lipopolysaccharide; IκBα, inhibitor of NF-Bα; p-, phosphorylated; DMSO, dimethyl sulfoxide; ctl, control.

were blocked with 5% skimmed milk in Tris-buffered saline in Tween-20 (TBST) buffer (10 mM Tris-base, 100 mM NaCl and 0.01% Tween-20) for 30 min at room temperature and then recognized with various primary antibodies (anti-iNOS, anti-TNF-α, anti-JNK, anti-phospho-c-JNK, anti-phospho-p44/p42 ERK, anti-phospho-p38 MAPK, anti-phospho-Akt, anti-phospho-p65, anti-p65, anti-IκBα, anti-ERK, anti-Akt, anti-p38 MAPK, anti-IL-1β or anti-α-tubulin; all, 1:1,000 in TBST) for 2 h at 4˚C prior to incubation with secondary antibody (HRP-conjugated anti-mouse IgG or anti-rabbit IgG) for 1 h at room temperature. The ECL system was used to detect the immunoreactive bands. Densitometry of the protein bands was performed using Biolight Windows Application, V2000.01 (Bio-Profil, VilberLourmat, France).

Statistical analysis. All results are expressed as the mean ± standard error of the mean and are accompanied by the number of observations (n). Multiple group comparisons were assessed using one-way analysis of variance followed by analysis using the Newman-Keuls method. P<0.05 was considered to indicate a statistically significant difference. Statistical analyses were performed using SAS (version 9.2; SAS Institute, Inc., Cary, NC, USA).

Results

Impact of TQ-5 on the viability and morphology of RAW 264.7 Cells. The toxicity of TQ-5 (Fig. 1A) was first examined in RAW 264.7 cells using the MTT assay. At concentrations of 10, 20 and 40 μM, TQ-5 alone or in the presence of LPS did not induce cytotoxicity in RAW 264.7 cells, as shown in Fig. 1B. This observation was further confirmed by examining the cell morphology, and the results revealed that normal macrophage cells exhibited a round morphology (Fig. 1C-a); by contrast, the LPS-stimulated cells exhibited an uneven morphology with pseudopodia formation and cell spreading (Fig. 1C-b). This modification was condensed by TQ-5 pretreatment, as shown in Fig. 1C-c. Additionally, TQ-5 at 40 μM did not prominently affect the normal round morphology of the LPS-stimulated cells, which exhibited a morphology identical to that of the unstimulated cells (Fig. 1C-d). This finding indicates that the effects of TQ-5 on RAW 264.7 cells are flexible and not cytotoxic.

Akt, but not MAPK, pathways are involved in mediating the effects of TQ-5 on reducing LPS-induced inflammation in RAW 264.7 macrophages. Previous studies have demonstrated that the MAPK and Akt signaling pathways are associated with LPS-induced inflammation in macrophages (22,23). Therefore, the potential involvement of these pathways in the TQ-5-mediated alleviation of LPS-induced inflammatory events was examined in the present study. The results indicated that LPS treatment significantly promoted the phosphorylation of JNK, p38 MAPK and ERK, in addition to Akt (Fig. 2A-D). However, the LPS-induced phosphorylation of MAPK was not completely abrogated by pretreatment with TQ-5; this metal complex inhibited the phosphorylation of Akt in a concentration-dependent manner. Therefore, TQ-5 suppressed the inflammatory responses by inactivating only Akt signaling pathways and not MAPK signaling pathways in LPS-stimulated RAW 264.7 macrophages.

TQ-5 normalizes the LPS-induced activation of NF-κB in RAW Cells. NF-κB is considered a prerequisite for the transcription

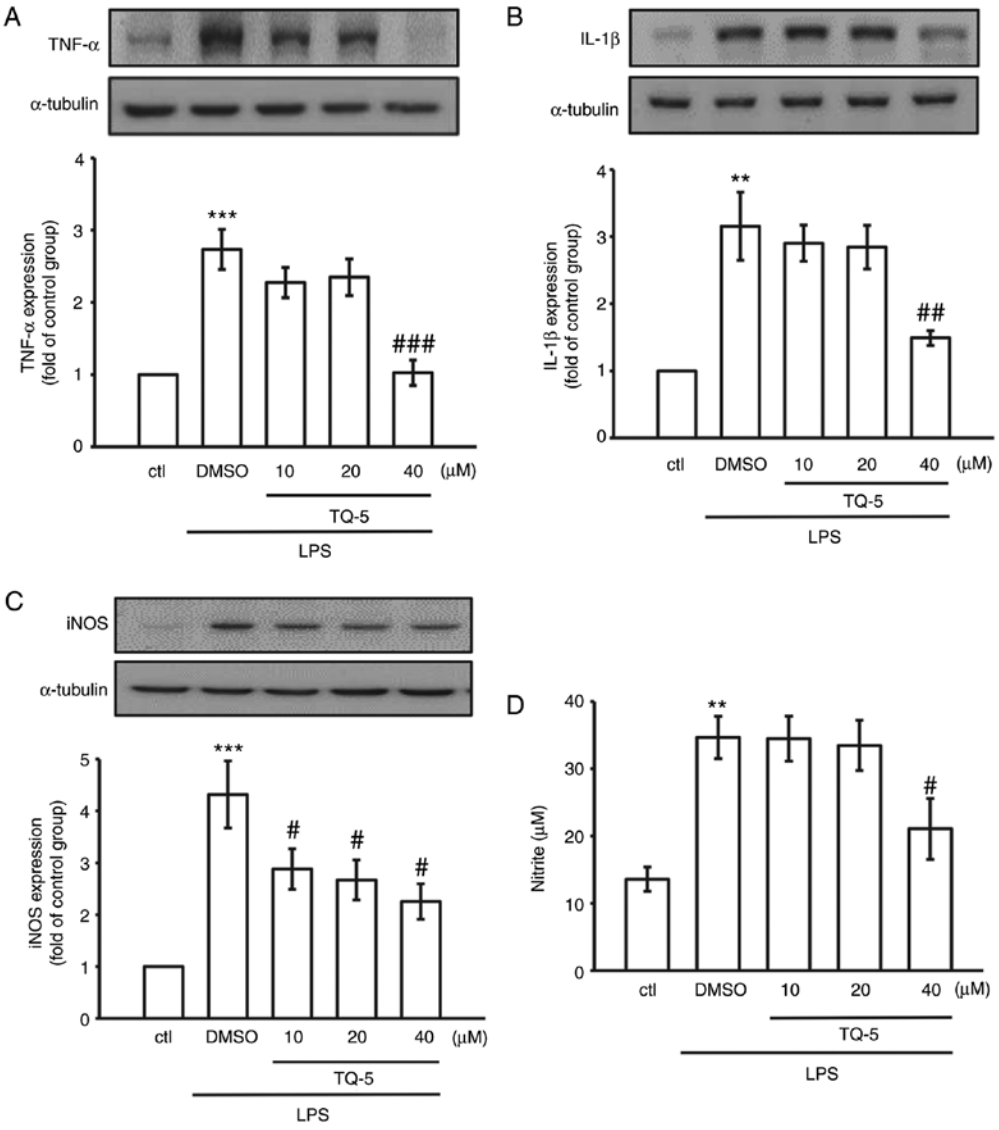

Figure 4. TQ-5 attenuates the LPS-induced expression of TNF-α, IL-1β and iNOS and production of NO in RAW cells. Cells were pretreated with TQ-5 (10, 20 and 40 μM) for 20 min and then stimulated by LPS (1 μg/ml) for 24 h. The protein levels of (A) TNF-α, (B) IL-1β and (C) iNOS were evaluated. (D) Cells were pretreated with TQ-5 (10, 20 and 40 μM) for 20 min and then stimulated by LPS (1 μg/ml) for 24 h. NO was measured using Griess reagent (1% sulfanilamide and 0.1% naphthalenediamine dissolved in 2.5% phosphoric acid). Data are presented as the mean ± SEM (n=4); **P<0.01 and ***P<0.001 compared with the ctl group; $^{\#}$P<0.05, $^{\#\#}$P<0.01 and $^{\#\#\#}$P<0.001 compared with the LPS group. LPS, lipopolysaccharide; TNF-α, tumor necrosis factor-α; IL-1β, interleukin-1β; iNOS, inducible nitric oxide synthase; NO, nitric oxide; DMSO, dimethyl sulfoxide; ctl, control.

of genes associated with inflammatory processes (22); therefore, the ability of TQ-5 to inhibit the activation of NF-κB was investigated in the present study. As shown in Fig. 3A, LPS evidently promoted the phosphorylation of NF-κB p65 with a concurrent degradation of IκBα after 30 min of exposure; therefore, this time point was selected for subsequent experiments. TQ-5 (40 μM) pretreatment markedly restored IκBα degradation (Fig. 3B) and effectively reduced the phosphorylation of NF-κBp65 (Fig. 3C) in the LPS-stimulated cells. These observations suggest that TQ-5 can act as a negative regulator of LPS-stimulated NF-κB activation in RAW 264.7 cells.

TQ-5 inhibits LPS-induced proinflammatory cytokines and mediators in RAW macrophages. To observe the effects of TQ-5 on the LPS-induced production of typical proinflammatory cytokines (TNF-α and IL-1β) and mediators (NO and iNOS) in RAW 264.7 cells, the cells were pretreated with various concentrations of TQ-5 (10, 20 and 40 μM) for 20 min. Subsequently, the cells were stimulated for 24 h with 1 μg/ml LPS. The proinflammatory cytokine (TNF-α and IL-1β) and mediator (iNOS) levels in the cellular supernatants were assessed using immunoblotting, and NO was examined using the Griess reagent. As indicated in Fig. 4A-D, the stimulation of RAW 264.7 cells with LPS alone significantly increased the expression levels of TNF-α, IL-1β and iNOS and the production of NO; however, these elevations were significantly reduced by TQ-5 at a maximum concentration of 40 μM. In addition, TQ-5 (40 μM) suppressed the LPS-stimulated mRNA expression of TNF-α, IL-1β and iNOS (Fig. 5A-C). These results suggest that TQ-5 inhibits the production of NO via the downregulation of iNOS and that the regulation of cytokine production serves a role in the TQ-5-mediated inhibition of inflammatory events in RAW cells.

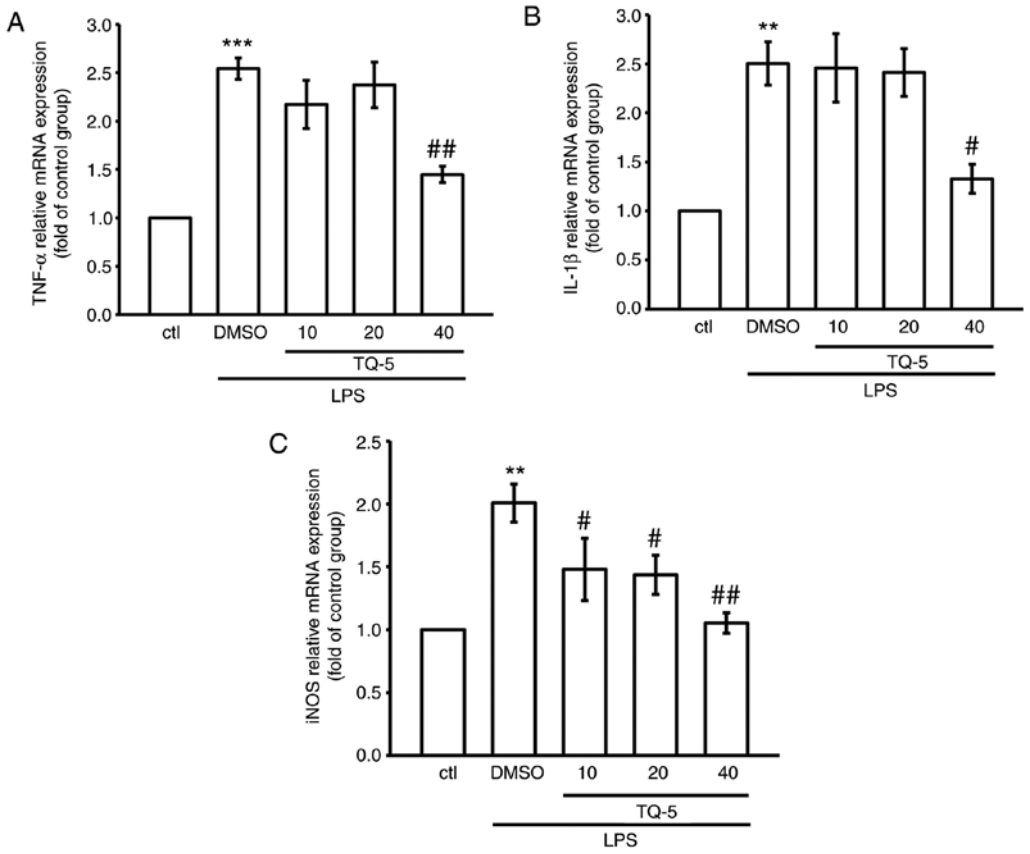

Figure 5. TQ-5 reduces the LPS-induced mRNA expression of TNF-α, IL-1β and iNOS in RAW cells. Cells were pretreated with TQ-5 (10, 20 and 40 μM) for 20 min and then stimulated by LPS (1 μg/ml) for 24 h. The mRNA expression levels of (A) TNF-α, (B) IL-1β and (C) iNOS were evaluated. Data are presented as the mean ± SEM (n=4); **P<0.01 and ***P<0.001 compared with the ctl group; $^{\#}$P<0.05 and $^{\#\#}$P<0.01 compared with the LPS group. LPS, lipopolysaccharide; TNF-α, tumor necrosis factor-α; IL-1β, interleukin-1β; iNOS, inducible nitric oxide synthase; DMSO, dimethyl sulfoxide; ctl, control.

TQ-5 attenuates acute liver injury in LPS-challenged mice. LPS-induced acute liver injury in mice is an extensively used model for investigating the mechanism of hepatoprotective and anti-inflammatory agents (24). To further establish the *in vitro* results of the effects of TQ-5 in inflammatory lesions, LPS was used to develop liver injury mouse models. Serum ALT and AST levels are vital indicators of liver dysfunction. Therefore, the levels of these enzymes were observed following LPS stimulation in the absence or presence of TQ-5. The body weight and survival rate was observed in mice of the treatment groups, as shown in Table SI. As shown in Fig. 6A and B, the intraperitoneal injection of 2.5 mg/kg LPS significantly increased serum ALT and AST levels, whereas TQ-5 treatment reduced these levels. LPS stimulated the expression of TNF-α, IL-1β, iNOS and p65 in the mouse liver (Fig. 6C-F). Consistent with the *in vitro* interpretations, downregulated phosphorylation of p65 and reduced expression levels of TNF-α, IL-1β and iNOS were confirmed as TQ-5-mediated *in vivo* protective effects. These results suggested that TQ-5 provided protection against liver injury by inhibiting inflammatory processes.

Discussion

The results of the present study demonstrated that TQ-5, a newly synthesized ruthenium metal complex, exhibited active anti-inflammatory property via impeding the LPS-induced inflammatory mediators (NO and iNOS), proinflammatory cytokines (TNF-α and IL-1β), Akt, phosphorylation of NF-κBp65 and degradation of IκBα in RAW 264.7 macrophages. In addition, this novel metal complex protected against liver injury in mice through suppressing the phosphorylation of p65 and consequently inhibited the expression of TNF-α, IL-1β and iNOS. These *in vivo* results are consistent with *in vitro* data and suggested that TQ-5 protected against liver injury by inhibiting the inflammatory processes induced by LPS. These data demonstrated that TQ-5 exhibited potent anti-inflammatory activity by mediating inhibition of the Akt/NF-κB signaling pathways; therefore, this metal complex may serve as a promising lead for the development of anti-inflammatory agents to treat acute liver failure. The RAW 264.7 cell line is one of the most commonly used cell lines for investigating inflammatory reactions as LPS can stimulate these cells and elicit the production of inflammatory mediators, including TNF-α, IL-6 and iNOS (25). In addition, the RAW264.7 cell line is exclusively competent for determining infection-related proinflammatory mediators (26). Initially, MTT assays were performed to measure the viability of RAW 264.7 cells and confirm that any anti-inflammatory effects of TQ-5 were not ascribed to decreasing RAW 264.7 cell viability (Fig. 1B). Based on these results, the concentrations of TQ-5 showing no cytotoxicity were selected for subsequent experiments.

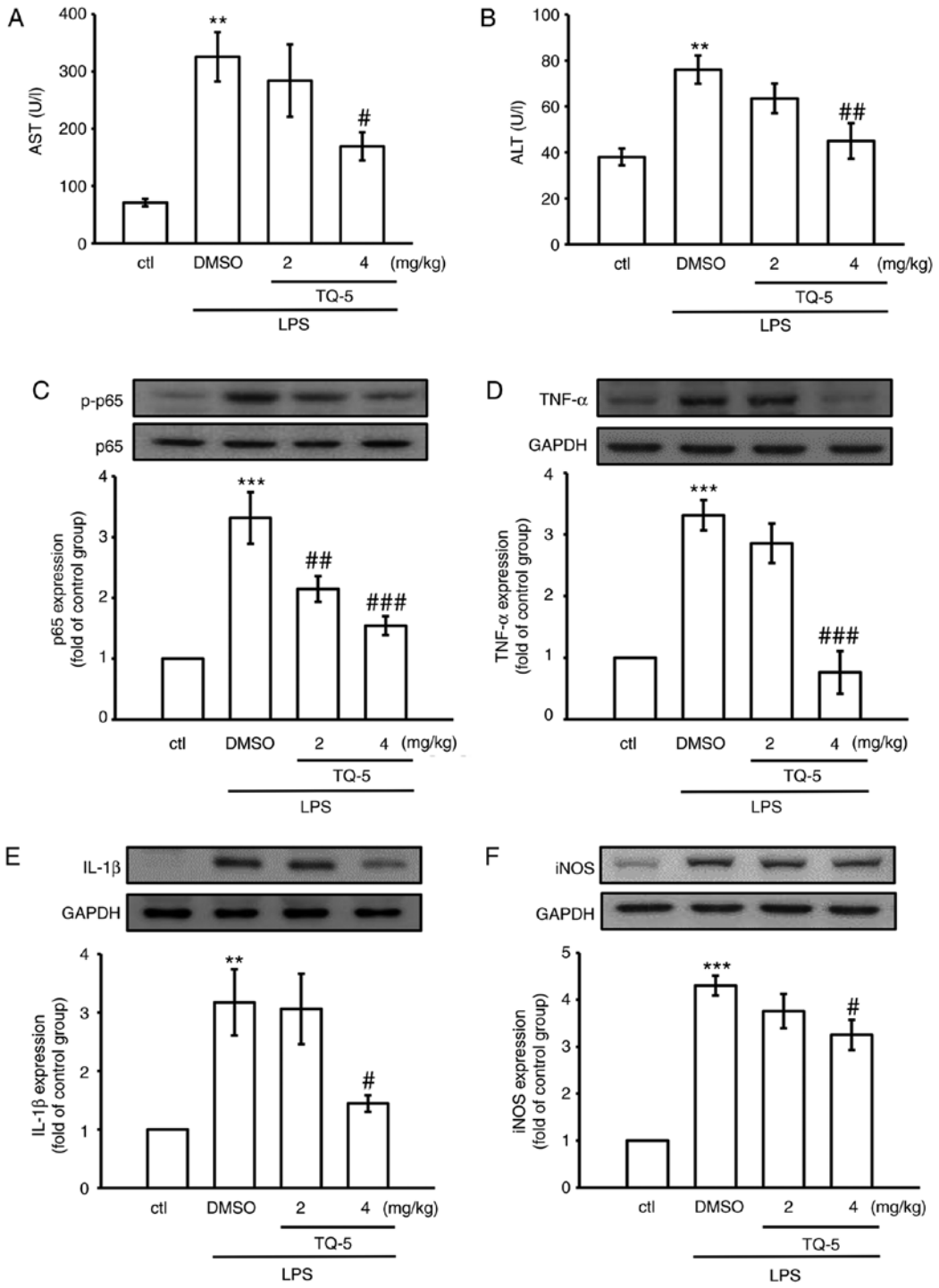

Figure 6. TQ-5 protects against LPS-induced liver injury in mice via inhibiting the expression of p-p65, TNF-α, IL-1β and iNOS. Mice were administered with an intraperitoneal injection of TQ-5 (2 and 4 mg/kg) 2 h prior to administration of LPS (2.5 mg/kg). After 6 h of LPS challenge, blood and liver tissues were collected to evaluate serum (A) AST and (B) ALT and the protein expression of (C) p-p65, (D) TNF-α, (E) IL-1β and (F) iNOS. Data are presented as the mean ± SEM (n=6); **P<0.01 and ***P<0.001 compared with the ctl group; $^{\#}$P<0.05, $^{\#\#}$P<0.01 and $^{\#\#\#}$P<0.001 compared with the LPS group. LPS, lipopolysaccharide; AST, aspartate aminotransferase; ALT, alanine aminotransferase; TNF-α, tumor necrosis factor-α; IL-1β, interleukin-1β; iNOS, inducible nitric oxide synthase; p-, phosphorylated; DMSO, dimethyl sulfoxide; ctl, control.

LPS triggered macrophages and subsequently produced proinflammatory mediators, including NO and iNOS, in addition to numerous cytokines, including TNF-α and IL-6 (27). Capillarisin, a natural flavonoid, reportedly inhibits the expression of iNOS in LPS-induced RAW 264.7 macrophages (28). Other studies have demonstrated that eight 2-phenylnaphthalenes (PNAP-1-8) inhibited the increment of iNOS expression and NO production in LPS-induced RAW 264.7 cells and suggested that the development of inflammation involves TNF-α (29). Hämäläinen *et al* (30) reported that kaempferol, a natural flavonol, inhibits the LPS-induced production of NO and expression of iNOS in activated macrophages. More appropriately, studies have reported that rhodium (III) complex inhibits the production of NO (31), and gold (I) complex

expressively reduces the production of TNF-α and IL-1β in LPS-activated macrophages (32). Similarly, the results of the present study showed that ruthenium complex TQ-5 reversed the LPS-induced elevation of TNF-α, IL-1β, NO and iNOS in RAW 264.7 cells. Therefore, these findings suggest that TQ-5 can inhibit inflammatory events by reducing the expression of iNOS, TNF-α and IL-1β and production of NO.

The NF-κB family serves vital roles in inflammation, immunity and survival. Upon LPS stimulation, IKK phosphorylates IκBα, leading to the nuclear translocation of NF-κB (33). The suppression of NF-κB activation by the flavonoid compounds capillarisin and genistein reportedly inhibits proinflammatory mediators iNOS, COX-II, TNF-α and IL-6 in LPS-stimulated RAW264.7 cells (34). In addition, one study demonstrated that pretreatment with phenylnaphthalenes PNAP-6 and PNAP-8 caused higher cytosolic levels of IκBα and NF-κBp65 in LPS-stimulated cells, thereby suppressing the translocation of NF-κBp65 to the nucleus (29). The copper complex (Cu^{2+}) was reported to inhibit the activation of NF-κB by preventing IκBα degradation in Jurkat T cells (35). Zinc and copper complexes have also been found to inhibit the activation of NF-κB in LPS-stimulated RAW 264.7 cells (36). In the present study, ruthenium complex TQ-5 inhibited the degradation of IκBα and phosphorylation of NF-κBp65 in LPS-induced RAW 264.7 macrophages. This finding suggested that TQ-5 inhibited LPS-induced proinflammatory mediators by regulating NF-κB signaling cascades.

In addition to NF-κB, MAPKs are induced by numerous extracellular stimuli, resulting in the downstream phosphorylation of crucial signaling molecules associated with inflammation (37). The MAPK family serves an essential role in LPS-induced inflammatory cytokine production in several cell types (38). In cells activated by LPS, the phosphorylation of MAPK is involved in activating the transcription factors of NF-κB and subsequently induces cytokine production (39). Another report describes that proinflammatory mediators are controlled by the downregulation of MAPK and NF-κB in LPS-treated RAW 264.7 cells (40). By contrast, the present study showed that pretreatment of RAW 264.7 cells with TQ-5 did not reduce the LPS-induced phosphorylation of p38 MAPK, JNK or ERK. However, the LPS-stimulated phosphorylation of Akt was concentration-dependently inhibited by TQ-5 in RAW 264.7 cells. Consistent with this result, a previous study demonstrated that myricetin, a natural flavonol, exhibits anti-inflammatory effects through inhibition of the Akt signaling pathway in LPS-induced RAW cells (41). This indicates that Akt pathways, but not MAPK-dependent pathways, are involved in the anti-inflammatory effect of TQ-5 on LPS-induced RAW cells.

The mouse LPS-induced acute liver injury model is one of the most frequently used research models. In the inflammatory event, LPS stimulates Kupffer cells to release TNF-α, IL-1β and IL-6; activates the NF-κB pathway; and successively increases the production of iNOS. These cellular signaling pathways serves vital roles in acute liver injury and inflammation (42,43). LPS also stimulates TNF-α, IL-6, and IL-1β in a model of ischemia-reperfusion liver injury (44,45). Therefore, it is hypothesized that the interference of LPS-induced inflammatory reactions may be advantageous for attenuating inflammation-associated liver disorders. In the present study, serum ALT and AST levels were measured to examine the effect of TQ-5 on liver injury. ALT is a specific marker for hepatic parenchymal injury, whereas AST is a nonspecific marker for hepatic injury. The results showed that TQ-5 ameliorated liver damage, as evidenced by the reduced levels of serum ALT and AST. The expression of hepatic NF-κB, TNF-α, IL-1β and iNOS were assessed to further identify the mechanism underlying the anti-inflammatory and hepatoprotective effects of TQ-5. TQ-5 significantly inhibited the LPS-induced hepatic expression of p-p65 and consequently reduced the expression of TNF-α, IL-1β and iNOS in the mouse liver. Together, these results suggest that TQ-5 impedes LPS-induced liver damage through the suppression of NF-κB, proinflammatory cytokines and mediators.

In conclusion, the anti-inflammatory and hepatoprotective effects of a newly synthesized novel ruthenium complex, TQ-5, were evaluated using LPS-stimulated RAW 264.7 cells and a mouse liver injury model, respectively. TQ-5 suppressed the LPS-induced production of NO, TNF-α, IL-1β and iNOS by inhibiting signaling molecules Akt and NF-κB in RAW 264.7 cells without inducing cytotoxicity. This novel metal complex exhibited defensive effects against LPS-induced liver injury *in vivo*. These findings suggest that TQ-5 may be a potential drug candidate for the development of anti-inflammatory agents to treat acute liver failure.

Acknowledgements

Not applicable.

Funding

This study was supported by grants from the Ministry of Science and Technology of Taiwan (grant nos. MOST 107-2314-B-195-002 and MOST 107-2221-E-195-001), the University Grants Commission, India (grant nos. MRP-MAJOR-CHEM-2013-5144; 69/2014 F. No. 10-11/12UGC), Cathay General Hospital (grant no. CGH-MR-A10715) and MacKay Memorial Hospital (grant no. MMH108-17).

Availability of data and materials

The datasets used and/or analyzed during the present study are available from the corresponding author on reasonable request.

Authors' contributions

TJ, KHL and YCL designed the study and wrote the manuscript. MV contributed to the chemical synthesis and analysis. SMH, CHH, CWH and CCC performed the experiments and analyzed the data. All authors contributed clarifications and guidance on the manuscript. All authors read and approved the final manuscript.

Ethics approval and consent to participate

All animal experiments and care procedures conformed to the Guide for the Care and Use of Laboratory Animals (LAC-2016-0395) and were approved by the Institutional

Animal Care and Use Committee of Taipei Medical University (Taipei, Taiwan).

Patient consent for publication

Not applicable.

Competing interests

The authors declare that they have no competing interests.

References

1. Denker SP, Ji S, Dingman A, Lee SY, Derugin N, Wendland MF and Vexler ZS: Macrophages are comprised of resident brain microglia not infiltrating peripheral monocytes acutely after neonatal stroke. J Neurochem 100: 893-904, 2007.
2. Kimbell B and Murray SA: What is the patient experience in advanced liver disease? A scoping review of the literature. BMJ Support Palliat Care 5: 471-480, 2015.
3. Newland CD: Acute liver failure. Pediatr Ann 45: e433-e438, 2016.
4. Kuroda N, Inoue K, Ikeda T, Hara Y, Wake K and Sato T: Apoptotic response through a high mobility box 1 protein-dependent mechanism in LPS/GalN-induced mouse liver failure and glycyrrhizin-mediated inhibition. PLoS One 9: e92884, 2014.
5. Moratalla A, Caparrós E, Juanola O, Portune K, Puig-Kröger A, Estrada-Capetillo L, Bellot P, Gómez-Hurtado I, Piñero P, Zapater P, *et al*: Bifidobacterium pseudocatenulatum CECT7765 induces an M2 anti-inflammatory transition in macrophages from patients with cirrhosis. J Hepatol 64: 135-145, 2016.
6. Jeong YH, Oh YC, Cho WK, Shin H, Lee KY and Ma JY: Anti-inflammatory effects of *Viola yedoensis* and the application of cell extraction methods for investigating bioactive constituents in macrophages. BMC Complement Altern Med 16: 180, 2016.
7. Dumitru CD, Ceci JD, Tsatsanis C, Kontoyiannis D, Stamatakis K, Lin JH, Patriotis C, Jenkins NA, Copeland NG, Kollias G and Tsichlis PN: TNF-alpha induction by LPS is regulated posttranscriptionally via a Tpl2/ERK-dependent pathway. Cell 103: 1071-1083, 2000.
8. Ho FM, Lai CC, Huang LJ, Kuo TC, Chao CM and Lin WW: The anti-inflammatory carbazole, LCY-2-CHO, inhibits lipopolysaccharide-induced inflammatory mediator expression through inhibition of the p38 mitogen-activated protein kinase signaling pathway in macrophages. Br J Pharmacol 141: 1037-1047, 2004.
9. Klintman D, Li X, Santen S, Schramm R, Jeppsson B and Thorlacius H: p38 mitogen-activated protein kinase-dependent chemokine production, leukocyte recruitment, and hepatocellular apoptosis in endotoxemic liver injury. Ann Surg 242: 830-838, 2005.
10. Bennett BL, Sasaki DT, Murray BW, O'Leary EC, Sakata ST, Xu W, Leisten JC, Motiwala A, Peirce S, Satoh Y, *et al*: SP600125, an anthrapyrazolone inhibitor of Jun N-terminal kinase. Proc Natl Acad Sci USA 98: 13681-13686, 2001.
11. DiDonato JA, Mercurio F and Karin M: Phosphorylation of I kappa B alpha precedes but is not sufficient for its dissociation from NF-kappa B. Mol Cell Biol 15: 1302-1311, 1995.
12. Tak PP and Firestein GS: NF-kappaB: A key role in inflammatory diseases. J Clin Invest 107: 7-11, 2001.
13. Cantley LC: The phosphoinositide 3-kinase pathway. Science 296: 1655-1657, 2002.
14. Guha M and Mackman N: The phosphatidylinositol 3-kinase-Akt pathway limits lipopolysaccharide activation of signaling pathways and expression of inflammatory mediators in human monocytic cells. J Biol Chem 277: 32124-32132, 2002.
15. Basri AM, Lord RM, Allison SJ, Rodríguez-Bárzano A, Lucas SJ, Janeway FD, Shepherd HJ, Pask CM, Philips RM and McGowan PC: Bis-picolinamide Ruthenium (III) dihalide complexes: Dichloride-to-diiodide exchange generates single trans isomers with high potency and cancer cell selectivity. Chemistry 23: 6341-6356, 2017.
16. Saeed HK, Saeed IQ, Buurma NJ and Thomas JA: The structure of linkers affects the DNA binding properties of tethered dinuclear Ruthenium (II) metallo-intercalators. Chemistry 23: 5467-5477, 2017.
17. Faller P and Hureau C: A bioinorganic view of Alzheimer's disease: When misplaced metal ions (re)direct the electrons to the wrong target. Chemistry 18: 15910-15920, 2012.
18. Hsia CH, Velusamy M, Sheu JR, Khamrang T, Jayakumar T, Lu WJ, Lin KH and Chang CC: A novel ruthenium (II)-derived organometallic compound, TQ-6, potently inhibits platelet aggregation: Ex vivo and in vivo studies. Sci Rep 7: 9556, 2017.
19. Jayakumar T, Hsu CY, Khamrang T, Hsia CH, Hsia CW, Manubolu M and Sheu JR: Possible molecular targets of novel ruthenium complexes in antiplatelet therapy. Int J Mol Sci 19: E1818, 2018.
20. Huang BP, Lin CH, Chen HM, Lin JT, Cheng YF and Kao SH: AMPK activation inhibits expression of proinflammatory mediators through downregulation of PI3K/p38 MAPK and NF-κB signaling in murine macrophages. DNA Cell Biol 34: 133-141, 2015.
21. Livak KJ and Schmittgen TD: Analysis of relative gene expression data using real-time quantitative PCR and the 2(-Delta Delta C(T)) method. Methods 25: 402-408, 2001.
22. Jung JS, Choi MJ, Lee YY, Moon BI, Park JS and Kim HS: Suppression of lipopolysaccharide-induced neuroinflammation by morin via MAPK, PI3K/Akt, and PKA/HO-1 signaling pathway modulation. J Agric Food Chem 65: 373-382, 2017.
23. Jing Y, Ai Q, Lin L, Dai J, Jia M, Zhou D, Che Q, Wan J, Jiang R and Zhang L: Protective effects of garcinol in mice with lipopolysaccharide/D-galactosamine-induced apoptotic liver injury. Int Immunopharmacol 19: 373-380, 2014.
24. Fan GW, Zhang Y, Jiang X, Zhu Y, Wang B, Su L, Cao W, Zhang H and Gao X: Anti-inflammatory activity of baicalein in LPS-stimulated RAW264.7 macrophages via estrogen receptor and NF-κB-dependent pathways. Inflammation 36: 1584-1591, 2013.
25. Hartley JW, Evans LH, Green KY, Naghashfar Z, Macias AR, Zerfas PM and Ward JM: Expression of infectious murine leukemia viruses by RAW264.7 cells, a potential complication for studies with a widely used mouse macrophage cell line. Retrovirology 5: 1, 2008.
26. Peng XX, Zhang SH, Wang XL, Ye TJ, Li H, Yan XF, Wei L, Wu ZP, Hu J, Zou CP, *et al*: Panax Notoginseng flower saponins (PNFS) inhibit LPS-stimulated NO overproduction and iNOS gene overexpression via the suppression of TLR4-mediated MAPK/NF-kappa B signaling pathways in RAW264.7 macrophages. Chin Med 10: 15, 2015.
27. Pan MH, Chiou YS, Tsai ML and Ho CT: Anti-inflammatory activity of traditional Chinese medicinal herbs. J Tradit Complement Med 1: 8-24, 2011.
28. Han S, Lee JH, Kim C, Nam D, Chung WS, Lee SG, Ahn KS, Cho SK, Cho M and Ahn KS: Capillarisin inhibits iNOS, COX-2 expression, and proinflammatory cytokines in LPS-induced RAW 264.7 macrophages via the suppression of ERK, JNK, and NF-κB activation. Immunopharmacol Immunotoxicol 35: 34-42, 2013.
29. Chang CF, Liao KC and Chen CH: 2-Phenylnaphthalene derivatives inhibit lipopolysaccharide-induced pro-inflammatory mediators by downregulating of MAPK/NF-κB pathways in RAW 264.7 macrophage cells. PLoS One 12: e0168945, 2017.
30. Hämäläinen M, Nieminen R, Vuorela P, Heinonen M and Moilanen E: Anti-inflammatory effects of flavonoids: Genistein, kaempferol, quercetin, and daidzein inhibit STAT-1 and NF-kappaB activations, whereas flavone, isorhamnetin, naringenin, and pelargonidin inhibit only NF-kappaB activation along with their inhibitory effect on iNOS expression and NO production in activated macrophages. Mediators Inflamm 2007: 45673, 2007.
31. Liu LJ, Lin S, Chan DS, Vong CT, Hoi PM, Wong CY, Ma DL and Leung CH: A rhodium (III) complex inhibits LPS-induced nitric oxide production and angiogenic activity in cellulo. J Inorg Biochem 140: 23-28, 2014.
32. Leung CH, Lin S, Zhong HJ and Ma DL: Metal complexes as potential modulators of inflammatory and autoimmune responses. Chem Sci 6: 871-884, 2015.
33. Chang CF, Chau YP, Kung HN and Lu KS: The lipopolysaccharide-induced pro-inflammatory response in RAW264.7 cells is attenuated by an unsaturated fatty acid-bovine serum albumin complex and enhanced by a saturated fatty acid-bovine serum albumin complex. Inflamm Res 61: 151-160, 2012.
34. Ji G, Zhang Y, Yang Q, Cheng S, Hao J, Zhao X and Jiang Z: Genistein suppresses LPS-induced inflammatory response through inhibiting NF-κB following AMP kinase activation in RAW 264.7 macrophages. PLoS One 7: e53101, 2012.

35. Satake H, Suzuki K, Aoki T, Otsuka M, Sugiura Y, Yamamoto T and Inoue J: Cupric ion blocks NF-kappa B activation through inhibiting the signal-induced phosphorylation of I kappa B alpha. Biochem Biophys Res Commun 216: 568-573, 1995.
36. Jeon KI, Jeong JY and Jue DM: Thiol-reactive metal compounds inhibit NF-kappa B activation by blocking I kappa B kinase. J Immunol 164: 5981-5989, 2000.
37. Kaminska B: MAPK signalling pathways as molecular targets for anti-inflammatory therapy-from molecular mechanisms to therapeutic benefits. Biochim Biophys Acta 1754: 253-262, 2005.
38. Zong Y, Sun L, Liu B, Deng YS, Zhan D, Chen YL, He Y, Liu J, Zhang ZJ, Sun J and Lu D: Resveratrol inhibits LPS-induced MAPKs activation via activation of the phosphatidylinositol 3-kinase pathway in murine RAW 264.7 macrophage cells. PLoS One 7: e44107, 2012.
39. Wang Z, Jiang W, Zhang Z, Qian M and Du B: Nitidine chloride inhibits LPS-induced inflammatory cytokines production via MAPK and NF-kappaB pathway in RAW 264.7 cells. J Ethnopharmacol 144: 145-150, 2012.
40. Intayoung P, Limtrakul P and Yodkeeree S: Antiinflammatory activities of crebanine by inhibition of NF κB and AP-1 activation through suppressing MAPKs and Akt signaling in LPS-induced RAW264.7 macrophages. Biol Pharm Bull 39: 54-61, 2016.
41. Hou W, Hu S, Su Z, Wang Q, Meng G, Guo T, Zhang J and Ga P: Myricetin attenuates LPS-induced inflammation in RAW 264.7 macrophages and mouse models. Future Med Chem 10: 2253-2264, 2018.
42. Karin M: Nuclear factor-kappa B in cancer development and progression. Nature 441: 431-436, 2006.
43. Chen F, Castranova V, Shi X and Demers LM: New insights into the role of nuclear factor-kappaB, a ubiquitous transcription factor in the initiation of diseases. Clin Chem 45: 7-17, 1999.
44. Colletti LM and Green M: Lung and liver injury following hepatic ischemia/reperfusion in the rat is increased by exogenous lipopolysaccharide which also increases hepatic TNF production in vivo and in vitro. Shock 16: 312-319, 2001.
45. Sheu JR, Chen ZC, Hsu MJ, Wang SH, Jung KW, Wu WF, Pan SH, Teng RD, Yang CH and Hsieh CY: CME-1, a novel polysaccharide, suppresses iNOS expression in lipopolysaccharide-stimulated macrophages through ceramide-initiated protein phosphatase 2A activation. J Cell Mol Med 22: 999-1013, 2018.